Polar Topside TEC Enhancement Revealed by Jason-2 Measurements

Xiaoqing Pi, Anthony J. Mannucci, and Olga Verkhoglyadova

Jet Propulsion Laboratory, California Institute of Technology

Corresponding author: Xiaoqing Pi (xiaoqing.pi@jpl.nasa.gov)

Key Points:

- NASA's Jason-2 satellite zenith-viewing GPS TEC measurements spanning 2008-2018 are analyzed.
- Significant localized increases of total electron content (TEC) above 1336 km altitude are reported for the first time.
- These polar topside TEC enhancements (PTTE) appear preferentially during southern summer.

Abstract

Polar topside total electron content (TEC) enhancement (PTTE) above 1336 km altitude is reported for the first time. The results are based on measurements from 2008 to 2018 made using a GPS receiver onboard NASA's Jason-2 satellite. The enhancement can exceed 5.5 TEC units or 78% relative to the dayside ambient state. Comparisons with COSMIC/FORMOSAT-3 topside TEC measurements confirm the PTTE events. Our statistical analysis reveals that PTTE mostly occurs in the southern dayside polar cap, with a seasonal preference of southern summer, regardless of geomagnetic conditions. Our case analysis indicates that PTTE is associated with the tongue of ionization. This suggests that the source of PTTE may be the dayside F region plasma that moves poleward following the anti-sunward plasma convection, and the plasma upflow driven by the polar wind may act to cause PTTE. The hemispheric asymmetry in PTTE occurrence remains to be a major unsolved puzzle.

Summary

Polar topside total electron content (TEC) enhancement (PTTE) above 1336 km altitude is reported for the first time. The results are based on measurements from 2008 to 2018 made using a GPS receiver onboard NASA's Jason-2 satellite. The observations show increasing occurrence of vertical PTTE towards the southern polar cap, with geomagnetic latitudes poleward of 65°S. The enhancement can exceed 5.5 TEC units (1 TECU = 10^{16} electrons/m^2) or 78% relative to the dayside ambient state. Comparisons with COSMIC/FORMOSAT-3 topside TEC measurements above 800 km altitude confirm the PTTE events. Our statistical analysis reveals that PTTE mostly occurs in the southern dayside polar cap, with a seasonal preference of southern summer, regardless of geomagnetic conditions. Our case analysis indicates that PTTE is associated with the tongue of ionization in the polar region. This suggests that the source of PTTE may be the dayside F region plasma that moves poleward following the anti-sunward plasma convection, and the plasma upflow driven by the polar wind may act to cause PTTE. The hemispheric asymmetry in PTTE occurrence remains to be a major unsolved puzzle.

1 Introduction

Ions above 1300 km altitude in the Earth's ionosphere and plasmasphere are mostly H^+ and He^+ as well as some O^+ near the lower altitudes at middle latitudes [e.g., Hagen and Hsu, 1975]. In the polar region, the photoionization is generally very weak due to large solar zenith angles, the plasma is no longer trapped in the plasmasphere, and H^+ as well as He^+ ion densities can be reduced by one order of magnitude compared with the densities at lower latitudes [e.g., Taylor et al., 1972]. Nominally, integrated electron densities or electron content above this altitude are lowest in the polar region compared with other latitudes.

We report a polar topside TEC enhancement (PTTE) phenomenon mostly seen in the south polar and polar cap region. The phenomenon is revealed in global positioning system (GPS) total electron content (TEC) data collected using a GPS receiver onboard the Jason-2 satellite. The nominally very low level of electron content makes it interesting to understand the source of PTTE. In this study we use a term topside TEC (briefly topTEC) to represent the vertical electron content between the Jason-2 orbit altitude (1336 km) and the GPS orbit altitude (20,200 km), unless specified otherwise. A global morphology of topTEC above 1336 km has been studied by Shim et al. [2017] using GPS data collected from the Jason-1 satellite. In their study the authors also noticed some slight increase of averaged topTEC with geomagnetic

activity in the south polar cap region, but details of the increase were not studied since the data were averaged over several similar solar and seasonal conditions.

2 Jason-2 GNSS Data and Processing

The Jason-2 satellite is an ocean surface topography mission jointly launched and operated by the NASA, the French space agency Centre National d'Études Spatiales (CNES), the NOAA, and the European Organization for the Exploitation of Meteorological Satellites (EUMETSAT). It was launched in June 2008 and decommissioned in October 2019. It is a successor to the TOPEX/Poseidon and Jason-1 ocean observing satellites. Further information about the Jason-2 mission including science instruments can be found in [Bannoura et al., 2005]. Among the sensors onboard are a GPS receiver with an upward-looking antenna to provide precise orbit ephemeris data. The same GPS data, including pseudorange and carrier phase of dual-frequency GPS signals at 1.57542 GHz (L1) and 1.2276 GHz (L2), can also be used to derive line-of-sight TEC.

The fundamental technique to derive TEC from these data is the same as the one that has been used widely in deriving TEC from ground-based GPS measurements, except that the flight receiver moves in its orbit rather than is fixed on the ground. The basic GPS data processing involves algebraically combining dual-frequency range and phase data to derive relative line-of-sight (LOS) TEC, leveling phase-derived TEC to range-derived TEC to remove the phase ambiguity, removing transmitter and receiver instrumental interfrequency biases from the range-derived LOS TEC data, and converting bias-removed slant TEC to vertical [e.g., Mannucci et al., 1998; Iijima et al., 1999; Stephens et al., 2011].

In our data processing, we removed the GPS transmitter biases from the Jason-2 LOS topTEC data using the biases derived from the daily processing of JPL's Global Ionospheric Map [Mannucci et al., 1998; Iijima et al., 1999]. Determination of the flight GPS receiver bias, however, involves the following additional processing and analysis. We compared the minimum topTEC measured by Jason-2 with estimates based on integrating satellite in-situ density measurements, and estimates obtained from an empirical ionosphere-plasmasphere model. First, a cumulative distribution function (CDF) method is used to identify the minimum relative LOS topTEC in the polar region under solar minimum conditions in January 2009. We then estimated the minimum topTEC by integrating the high-latitude measurements of the Akebono satellite during winter nighttime in the polar region [Kitamura et al., 2009]. The Akebono satellite provides in-situ electron densities in an altitude range of 274 km to 10,500 km, and our estimation of topTEC includes density extrapolation up to 20,200 km. The minimum topTEC was also estimated using the Global Core Plasma Model (GCPM) [Gallagher et al., 2000]. A number of model outputs at 66 deg <= latitude <= 68 deg, magnetic local time > 1800 or < 0600 are averaged for solar minimum conditions specified with inputs for the solar 10.7 cm radio flux index F10.7 = 65.5 and the planetary daily magnetic index Ap = 0^+ (e.g., ftp://ftp.swpc.noaa.gov/pub/indices/old_indices/). Both Akebono and GCPM estimates suggest a vertical TEC level of about 0.15 TECU above 1336 km. The receiver bias is then determined from the difference between the estimated and the Jason-2 LOS measurements.

In this study, topside line-of-sight TEC measurements are all converted to vertical. The conversion is performed using the following geometric mapping function,

$$M(z) = \frac{ds}{dh} = \frac{1 + r_s/r_o}{cos(z) + \sqrt{(r_s/r_o)^2 - sin(z)^2}},$$

where z is the observation zenith angle, *dh* is the vertical distance from the orbit to the sub-plasmaspheric point where the plasmasphere is approximately represented using a shell, *ds* represents the slant range from the satellite to the shell along the ray path, r_s is the geocentric radius of the shell, and r_o is the geocentric radius of the satellite. This mapping function was proposed for tropospheric measurements by Foelsche and Kirchengast [2002]. Zhong et al. [2016] compared the mapping errors of this function with a few others and found that this function would yield less error if an electron density centroid height is chosen for the shell height. For the Jason-2 orbit, the estimate of plasmaspheric centroid height is obtained as follows,

$$h_c = \frac{\int_{h_{LEO}}^{h_{GPS}} n_e h dh}{\int_{h_{LEO}}^{h_{GPS}} n_e dh},$$

where n_e denotes electron density. Using GCPM, the estimated centroid height is approximately 3500 km [Zhong et al., 2016]. In addition to the selections of mapping function and centroid height, we also applied a 30° zenith cutoff to exclude the data at larger zenith angles in order to reduce mapping errors.

3 Observations and TEC Enhancement

In examination of topTEC data during the first day of the 2013 St. Patrick's storm (17 March 2013), we first noticed a phenomenon that topTEC increases with latitude in the south polar cap (poleward of roughly -65° magnetic latitude). Figure 1 shows Jason-2 topTEC data during the whole day vs. quasi-dipole geomagnetic latitude [Richmond, 1995]. Observations from all GPS satellites at and above 60° elevation angle (= 90° – zenith angle) for the day are over plotted in the figure. In this data set, most of the topTEC data show a latitudinal pattern that gradually decreases with increasing latitude. Surprisingly an opposite variation trend is observed in several observation tracks in the southern polar region from about -60° to -80° geomagnetic latitude. topTEC around -70° increases to levels of about 12.6 TECU, which is an approximately 78% increase compared with about 7 TECU of the ambient state at lower latitudes near -55°. Interestingly the data in the northern hemisphere also shows the opposite variation trend in an observation track, but the locations of the topTEC enhancement are at lower latitudes roughly between 45° and 59° and TEC increases to about 8.5 TECU near 55° magnetic latitude, which is much weaker than what are observed in the antarctic region.

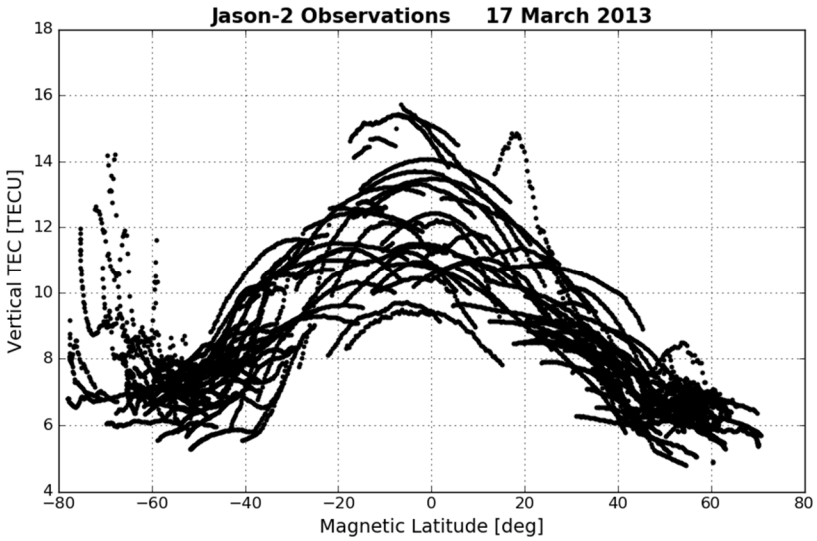

Figure 1. TEC above 1336 km altitude observed during 17 March 2013 using the GPS receiver with upward-looking antenna onboard the Jason-2 satellite. The polar topside TEC enhancement (PTTE) appears in the southern hemisphere at magnetic latitudes poleward of -60°.

To validate the measurements, we examined topTEC data collected during the same day using GPS receivers onboard COSMIC/FORMOSAT-3 satellites [e.g., Lee and Rocken, 2000] orbiting at about 800 km altitude. Five of the six COSMIC satellites were operating on 17 March 2013. We find that PTTE also appears in several COSMIC observation tracks, in which TEC increases to 13 TECU from the ambient 8.2 TECU (increasing by 59%). Figure 2 presents the Jason-2 and COSMIC PTTE events vs. magnetic latitude (MLAT) and magnetic local time (MLT) with the same elevation limit of 30 degrees. Being aware that the COSMIC topTEC observations include also electron density contribution between 800 km and 1336 km, we also notice the following differences in comparing the PTTE events between the Jason-2 and COSMIC observations: (1) the UT difference is about two hours: Jason-2 observations are made during ~0645 – 0715 UT, while the COSMIC observations are made during 0842 – 0900 UT; (2) although the events are observed at similar latitudes, the PTTE events appear in different local time sectors, the Jason-2 observations being between ~0810-1015 MLT and ~13-16 MLT, while the COSMIC observations being between ~1240-1345 MLT; (3) although topTEC is structured horizontally, the structures captured by the two LEOs are different, which is probably due to different MLT sectors. The COSMIC data in the northern polar region is also examined, in which we find an apparent PTTE with about 3 TECU increase from the ambient topTEC between 50 and 60° MLAT and 2015~2100 MLT during 1209-1213 UT, but the northern event (not shown here) does not match the southern ones in terms of UT, MLT, and MLAT. Nevertheless, PTTE appears in both Jason-2 and COSMIC satellite data within about 2 hours (UT) on the same day in the south polar cap at similar latitudes, and the events occur during daytime in morning and following sectors.

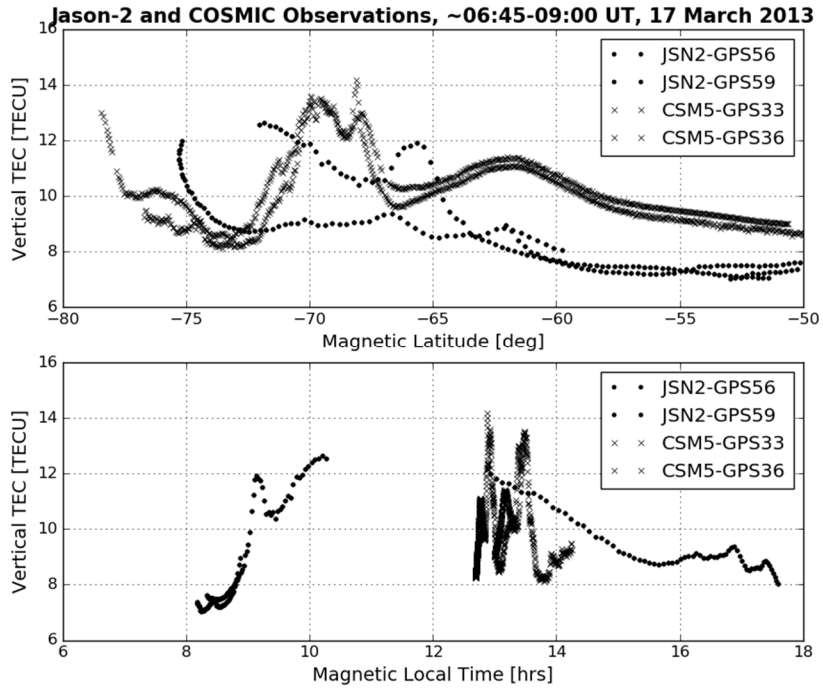

Figure 2. PTTEs observed during 17 March 2013 using the GPS receivers with upward-looking antennas onboard the Jason-2 satellite (filled circles) and one of the COSMIC satellites (crosses). The PTTE data are also presented vs. magnetic local time (bottom panel). The plotted Jason-2 observations are made during ~0645 – 0715 UT, and the COSMIC observations are made during 0842 – 0900 UT.

4 MLAT-MLT Patterns, and Seasonal as well as Hemispheric Asymmetry of PTTE

To investigate MLAT and MLT patterns of PTTE, we analyzed the Jason-2 topTEC data during November 2008 through October 2019. Data from 2717 days spanning these years are included in this study after excluding days during 2009 and 2010 as well as other days concerning data quality. A solar cycle effect on the base level of topTEC is removed by the following method: the minimum value of topTEC data within each period of 27 consecutive days is removed from topTEC data, which should remove the effect that follows the synodic solar rotation period. We then binned all data in both polar regions in a quasi-equal area (QEA) grid. The grid is constructed to minimize an effect of the nominal polar grid that makes the surface areas of polar pixels smaller at latitudes approaching pole. The QEA grid sets the azimuthal arc length of MLT bins approximately equal between different MLATs. This yields different numbers of MLT bins at different latitudes but the pixel surface areas are approximately similar at all latitudes. Figure 3 shows the maximum values of the detrended topTEC data during the 11 years on the QEA grid, in which the azimuthal arc length in MLT dimension ranges from 250 km to 291 km, and the latitude spacing in radial dimension (MLAT) is 2.5 deg. In each QEA pixel where data are available, the maximum topTEC value is determined among at least 5 data samples, and the number of data samples ranges from 5 to ~10000. The maximum of topTEC data in the polar regions of two hemispheres are color-coded and displayed in separate panels. We notice that there are less data samples in the northern polar cap than the data samples in the southern polar cap. This may be attributed to the offset of the geomagnetic pole from the

geographic pole and the Jason-2 orbit geometry. The orbit design follows the geographic system while the plot shows data in the magnetic system.

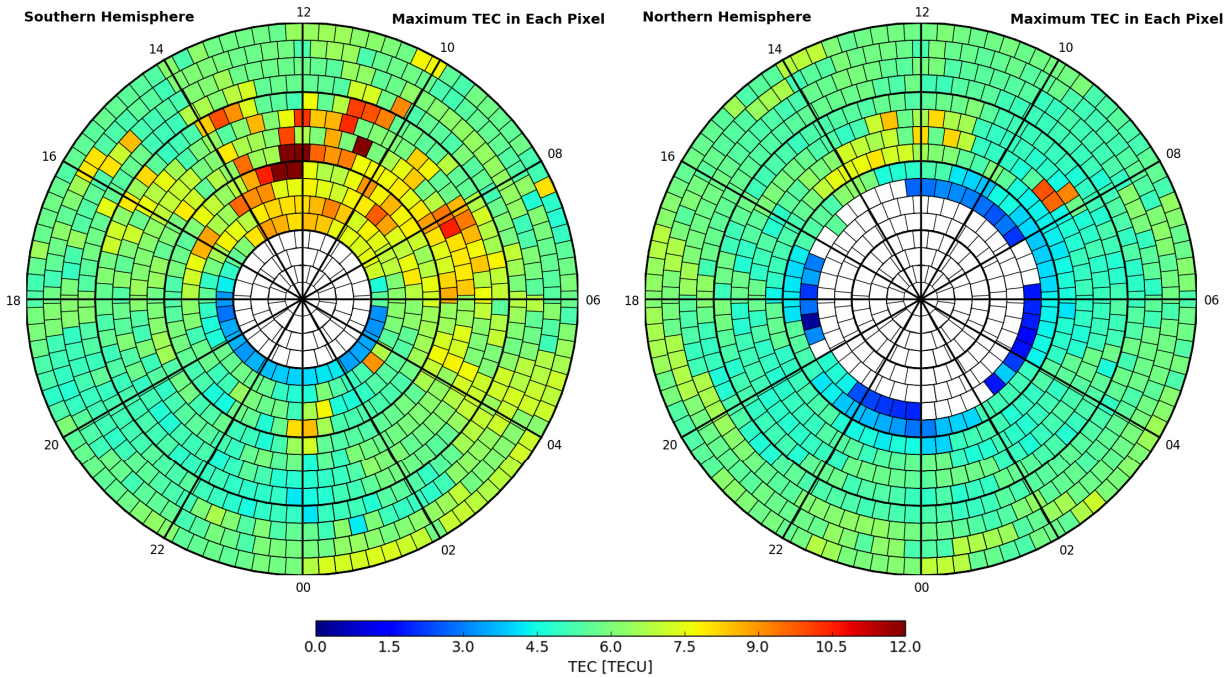

Figure 3. The maximum of topTEC values from solar-cycle detrended Jason-2 GPS TEC data from 2717 days during 2008–2019. The data are displayed in the polar QEA grid (referring to the text of this manuscript) constructed with MLAT (radial) and MLT (azimuthal) coordinates. The outermost MLAT is 50°. The white pixels indicate that the number of data samples is less than 5 or the data are not available in the bins.

Examining Jason-2 topTEC data we notice several characteristics of PTTE: (1) in the southern polar cap, quite many relatively large PTTE values can be found at MLAT higher than 65°S; (2) PTTE mostly appears on the dayside between 6 and 16 MLT; (3) PTTE can occur during either geomagnetically disturbed or quiet days (Table 1); (4) PTTE in the southern polar region occurs more frequently in November through February than in other months (Figure 4). The number of PTTE events included in (3) and (4) analyses is obtained using the following method: if the maximum range (from minimum to maximum) of solar-cycle-detrended topTEC measurements during a day reaches or exceeds 4 TECU at magnetic latitudes higher than |65|°, that day is counted as a single event. This threshold emphasizes rather strong effects and may exclude many weak events, and it does not count multiple events during the same day. The number of events under different geomagnetic conditions is summarized as follows (where Ap is the daily planetary geomagnetic index):

- Northern hemisphere: 18 events for Ap < 10, 13 events for 10 <= Ap < 20, and 9 events for Ap >= 20.
- Southern hemisphere: 190 events for Ap < 10, 82 events for 10 <= Ap < 20, and 77 events for Ap >= 20.

The number of events in different seasons is summarized in Figure 4.

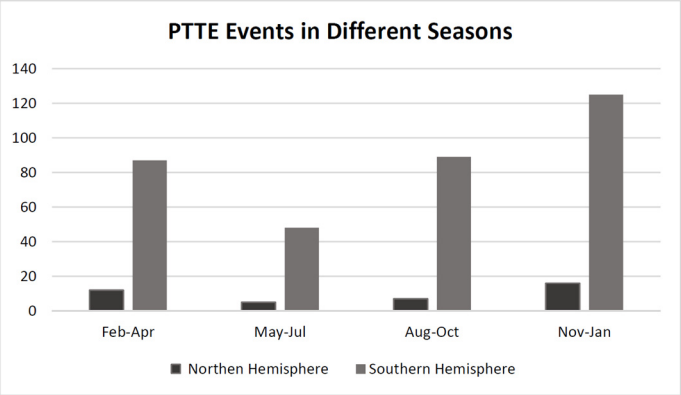

Figure 4. Observed PTTE events in different seasons.

4 Discussion About the Source of PTTE

Two questions about PTTE are its plasma source and the mechanism that drives the plasma to the altitude region where plasma density is nominally very low. The polar wind is a potential candidate that characterizes plasma upflows in the polar region and may cause PTTE. The modeling study by Schunk and Sojka [1997] has suggested that at times O^+ can remain the dominant ion to very high altitudes in the polar cap, where the magnetic field is in the open field domain. The modeling study has shown that significant enhancement in electron and ion temperature as well as field-aligned O^+ velocity can be associated with the polar wind. Our observations indicate that the dayside PTTE mostly occurs between 0600 and 1600 MLT, which seems consistent with the modeling prediction.

Horizontally, O^+ dominant plasma at ionospheric altitudes can flow from the dayside into the polar cap following the anti-sunward flow of plasma convection. A familiar ionospheric feature associated with this plasma flow is the tongue of ionization (TOI) [e.g., Sato, 1959; Knudsen, 1974; Sojka et al., 1994; Foster et al., 2005]. In order to investigate ambient ionospheric structures that may be associated with PTTE, we have examined ground-based GPS TEC measurements during 17 March 2013, which are available at the CEDAR Madrigal database (http://cedar.openmadrigal.org/single/). Figure 5 shows the TEC data at 0645-0700 UT and 0845-0900 UT intervals in the south polar region. During 0645-0700 UT the ground-based GPS measurements show TEC enhancement at magnetic latitudes poleward of 65°S in the 08-09 MLT and adjacent sectors. The MLAT and MLT sectors match those at which the Jason-2 PTTE is observed. During the 0845-0900 UT interval, although there is a data gap in the ground-based data at 67.5°S ~ 72°S magnetic latitudes and ~13 MLT where COSMIC PTTE is present (Figure 2), the nearby surrounding ground-based measurements also show TEC enhancement. The correlation between the PTTE events above 1336 km or 800 km and the ground-based TEC observations at the two intervals suggest that dayside plasma from lower latitudes may have moved into the polar cap. We also attempted to find plasma density and drift data from the Defense Meteorology Satellite Program (DMSP) to further verify our assessment, but unfortunately the available DMSP observations do not match the times and locations of the Jason-2 and COSMIC measurements.

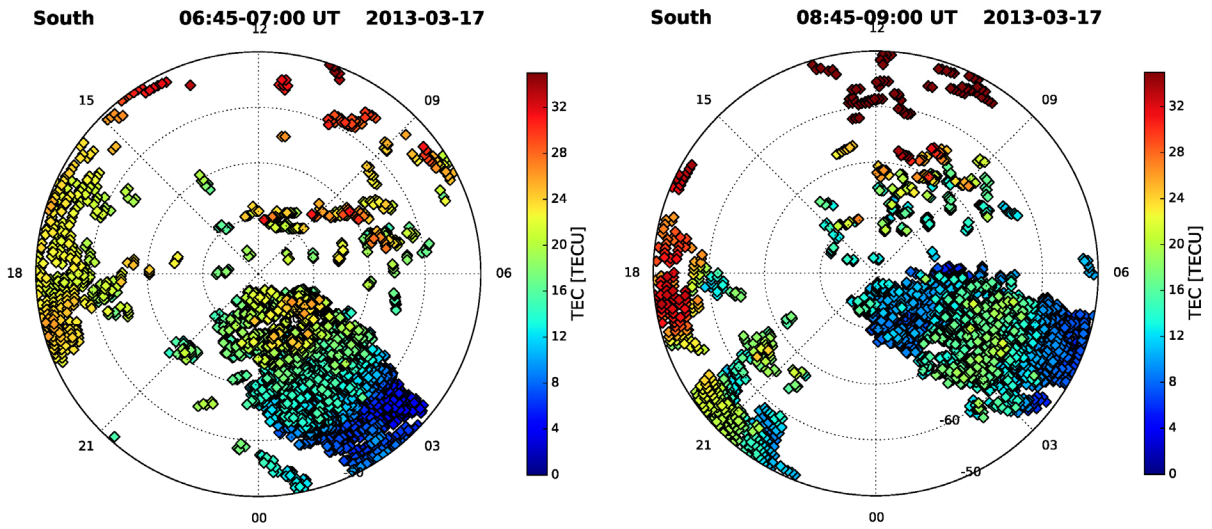

Figure 5. Ground-based TEC observations over the south polar region in a magnetic latitude (radial) and magnetic local time (azimuthal) coordinate system for two UT intervals during 17 March 2013. The outmost magnetic latitude is -50°.

5 Conclusions

A PTTE phenomenon is revealed in the Jason-2 satellite upward-looking GPS observations for the first time. It presents significant TEC enhancements relative to background above 1336 km altitude in the south polar cap region. Jason-2 PTTE events are corroborated in the south polar cap by COSMIC topside GPS TEC measurements on 17 March 2013 when Jason-2 PTTE is observed, though the measurements made by the two satellites are at slightly different MLT sectors (separated by ~4 hours) and about 2 hours different in UT. The TEC reaches as high as 12.5 to 13 TECU during the PTTE events, which are about 78% and 59% above the ambient background respectively for the Jason-2 and COSMIC measurements. Such enhancements are significant in the polar cap region where electron density and TEC levels are normally very low. The data set spanning 8 years were analyzed using a specially-developed quasi-equal area grid approach. Our analysis of Jason-2 topTEC data during November 2008 through October 2019 (data in 2009 and 2010 are not included concerning the data quality) reveals the following characteristics:

1. PTTE events are observed in the polar region near or higher than 65° MLAT, much more frequently in the southern polar region than in the northern polar region.
2. Observations show that the TEC increase above 1336 km can reach 12.5 TECU, increasing 78% above the ambient state.
3. The phenomenon is mostly observed on the dayside between 6 and 16 MLT.
4. The events can occur during either magnetically disturbed or quiet days.
5. In the southern polar region, PTTE is observed more frequently during summer season (November through February) than other seasons.

A case analysis shows that PTTE occurs alongside an enhancement in ground-based TEC measurements, which appears to be associated with the tongue of ionization. This leads to our

suggestion that a source of PTTE may be the dayside F region plasma that advects to higher latitudes following the anti-sunward plasma convection, and the plasma upflows caused by the polar wind may act to increase the topside plasma density. However, the hemispheric asymmetry in PTTE occurrence remains to be the major unsolved puzzle.

Acknowledgments

The research was carried out at the Jet Propulsion Laboratory, California Institute of Technology, under a contract with the National Aeronautics and Space Administration (80NM0018D0004).. Sponsorship of the NASA Living With a Star program is gratefully acknowledged. The authors are grateful to the Jason-2 mission management, the University Corporation for Atmospheric Research, the Taiwan National Space Program Office, and Dr. Anthea Coster for making measurements from Jason-2, COSMIC/FORMOSAT-3, and ground-based GNSS data available to research communities. The authors are grateful to Shailen Desai at the Jet Propulsion Laboratory for helpful discussions of Jason-2 data processing. The Jason-2 GNSS data are accessible at https://www.bou.class.noaa.gov/saa/products/search?datatype_family=JASON-ORB. The COSMIC data archive is accessible at https://cdaac-www.cosmic.ucar.edu/cdaac/products.html#cosmic. The CEDAR Madrigal database is accessible at http://cedar.openmadrigal.org/single/.

References

Bannoura, W. J., Wade, A. and Srinivas, D. N. (2005), "NOAA Ocean Surface Topography Mission Jason-2 project overview," Proceedings of OCEANS 2005 MTS/IEEE, Washington, DC, 2005, pp. 2155-2159 Vol. 3, doi: 10.1109/OCEANS.2005.1640083.

Bellchambers, W. H., and Piggott, W. R. (1958), Ionospheric measurements made at Halley Bay, Nature, Vol.182, No.4649, pp.1596-1597.

Foelsche U, Kirchengast G (2002) A simple ‘‘geometric’’ mapping function for the hydrostatic delay at radio frequencies and assessment of its performance. Geophys Res Lett 29:1473. doi:10.1029/2001GL013744

Foster, J. C., et al. (2005), Multiradar observations of the polar tongue of ionization, J. Geophys. Res., 110, A09S31, doi:10.1029/2004JA010928.

Gallagher, D. L., Craven, P. D., and R. H. Comfort (2000), Global core plasma model, J. Geophys. Res., Vol.105, No.A8, pp.18819-18833.

Hagen, J. B., and Hsu, P. Y-S. (1975), The structure of the protonosphere above Arecibo, J. Geophys. Res., Vo.79, No.28, pp.4269-4275.

Iijima, B. A., Harris, I. L., Ho, C. M., Lindqwister, U. J., Mannucci, A. J., Pi, X., Reyes, M. J., Sparks, L. C., Wilson, B. D. (1999), Automated daily process for global ionospheric total electron content maps and satellite ocean altimeter ionospheric calibration based on Global Positioning System data, Journal of Atmospheric and Solar-Terrestrial Physics, Vo.61, Issue 16, pp.1205-1218.

L.C. Lee, C. Rocken, "Applications of Constellation Observing System for Meteorology, Ionosphere & Climate", R. Kursinski (Ed.), Springer, 2000, ISBN 962-430-135-2

Knudsen, W. C. (1974), Magnetospheric convection and high-latitude F_2 ionosphere, J. Geophys. Res., Vol.79, No.7.

Kitamura, N., A. Shinbori, Y. Nishimura, T. Ono, M. Iizima, and A. Kumamoto (2009), Seasonal variations of the electron density distribution in the polar region during

geomagnetically quiet periods near solar maximum, J. Geophys. Res., 114, A01206, doi:10.1029/2008JA013288.

Mannucci, A. J., B. D. Wilson, D. N. Yuan, C. H. Ho, U. J. Lindqwister, and T. F. Runge (1998), A global mapping technique for GPS-derived ionospheric total electron content measurements, *Radio Sci.*, *33*(3), 565–582, doi:10.1029/97rs02707.

Richmond, A. D., Ionospheric Electrodynamics Using Magnetic Apex Coordinates, J. Geomag. Geoelectr., 47, 191-212, 1995.

Sato, T. (1959), Morphology of ionospheric F_2 region disturbances in the polar regions, Rep. Ionos. Res. Space Res., Japan, 13, 91.

Schunk, R. W., and Sojka, J. J., (1997), Global ionosphere-polar wind system during changing magnetic activity, J. Geophys. Res., Vol.102, No. A6, pp.11625-11651.

Shim, J. S., G. Jee, and L. Scherliess (2017), Climatology of plasmaspheric total electron content obtained from Jason 1 satellite, J. Geophys. Res. Space Physics, 122, doi:10.1002/2016JA023444.

Sojka, J. J., Bowline, M. D., Schunk, R. W. (1994), Patches in the polar ionosphere: UT and seasonal dependence, J. Geophys. Res., Vol.99, No. A8, pp.14959-14970.

Stephens, P., A. Komjathy, B. Wilson, and A. Mannucci (2011), New leveling and bias estimation algorithms for processing COSMIC/FORMOSAT-3 data for slant total electron content measurements, Radio Sci., 46, RS0D10, doi:10.1029/2010RS004588.

Taylor Jr., H. A., and Walsh, W. J. (1972), The light-ion trough, the main trough, and the plasmapause, J. Geophys. Res., Vol. 77, No.34, pp.6716-6723.

Zhong, J., Lei, J., Dou, X., and Yue, X. (2016), Assessment of vertical TEC mapping functions for space-based GNSS observations, GPS Solut (2016) 20:353–362, DOI 10.1007/s10291-015-0444-6